Biomedical Science Letters 2015, 21(1): 23~31
http://dx.doi.org/10.15616/BSL.2015.21.1.23
eISSN : 2288-7415

Original Article

The Characterization of Anti-HER-2/*neu* Monoclonal Antibody using Different *in vivo* Imaging Techniques

Cheol Moon[1], Eun Jung Kim[2], Dan Bee Choi[2], Byoung Soo Kim[2], Sa Hyun Kim[1] and Tae Hyun Choi[2,†]

[1]Department of Clinical Laboratory Science, Semyung University, Jecheon 390-711, Korea
[2]Molecular Imaging Research Center, Korea Institute of Radiological and Medical Sciences (KIRAMS), Seoul 139-706, Korea

Recently, specific antibodies have been used extensively to diagnose and treat various diseases. It is essential to assess the efficacy and specificity of antibodies, especially the *in vivo* environment. Anti-HER-2/*neu* mAb was evaluated as a possible transporting agent for radioimmunotherapy. The monoclonal antibody was successfully radio-labeled with ^{131}I. *In vitro* binding assays were performed to confirm its targeting ability using another radio-iodine, ^{125}I. Binding percentage of ^{125}I labeled anti-HER-2/*neu* mAb in HER-2/*neu* expressing CT-26 cells was found to be 4.5%, whereas the binding percentage of ^{125}I labeled anti-HER-2/*neu* mAb in wild-type CT-26 was only 0.45%. *In vivo* images were obtained and analyzed through γ-camera and an optical fluorescent modality, IVIS-200. γ-camera images showed that ^{131}I labeled anti-HER-2/*neu* mAb accumulated in HER-2/*neu* CT-26 tumors. Optical imaging based on near infrared fluorescence labeled anti-HER-2/*neu* mAb showed higher fluorescence intensities in HER-2/*neu* CT-26 tumors than in wild-type CT-26 tumors. Anti-HER-2/*neu* mAb was found to specifically bind to its receptor expressing tumor. Our study demonstrates that *in vivo* imaging technique is a useful method for the evaluation of an antibody's therapeutic and diagnostic potentials.

Key Words: Radioimmunotherapy (RIT); *In vivo* imaging; Monoclonal antibody; HER-2/*neu* oncogene

INTRODUCTION

Tumor targeting by radiolabeled mAb is an attractive approach to cancer treatment (Fani et al., 2002). RIT is a form of targeted therapy that uses parent mAbs to deliver radioactivity, which is emitted by a conjugated radioisotope, to antigen positive tissues (Kraeber-Bodéré et al., 2014). Tumor cells are damaged by the combined effects of the antibody and ionizing radiation (Read ED, 2014). Moreover, tumor cells not bound by antibody may still be affected by radiation from adjacent cells, due to cross-fire (Shimoni and Nagler, 2007). During the past few years, the U.S. Food and Drug Administration approved two RIT pharmaceuticals for the treatment of non-Hodgkin's lymphoma, i.e., the anti-CD20 monoclonal antibodies, ^{90}Y-ibritumomab tiuxetan (Zevalin) and ^{131}I-tositumomab (Bexxar). Moreover, several new radioimmunoconjugates are currently being evaluated in clinical trials (Sharkey and Goldenberg, 2005). Therapeutic radionuclides usually emit β-particles to the tumor (Fani et al., 2002). ^{131}I is one of the radionuclides mostly used for RIT (Lewington V, 2005). However, recently, instead of ^{131}I, ^{90}Y is used for RIT studies because of pure β emission (DeNardo GL, 2000), and its β particles penetrate more effectively than ^{131}I (Esteban JM, 1990). However, as ^{90}Y does not emit gamma rays, the *in vivo* distribution of

*Received: February 1, 2015 / Accepted: March 13, 2015
†Corresponding author: Tae Hyun Choi. Molecular Imaging Research Center, Korea Institute of Radiological and Medical Sciences (KIRAMS), Seoul 139-706, Korea.
Tel: +82-2-970-1489, Fax: +82-2-970-2435
e-mail: thchoi@kirams.re.kr

^{90}Y-labeled antibody cannot be visualized (Wiseman GA, 2000). Some target antigens (e.g. HER-1, dHER-2/*neu*) are internalized by cells after antibody binding (Jaramillo et al., 2006). Moreover, ^{90}Y is a radiometal that is retained intracellularly, whereas ^{131}I is released from cells by deiodination (Witzig TE, 2006). ^{186}Re is another metallic radionuclide suitable for RIT. It emits both β and γ radiation. These γ rays, which are emitted in only 9% of the disintegrations, are of low energy (137 keV) whereas β emissions are of medium energy (mean 362 keV) (van Gog FB et al., 1997). ^{67}Cu is also a possibility for RIT and provides low energy β emissions (average 141 keV) and medium energy gamma rays (185 keV) which are suitable for imaging (DeNardo et al., 1999).

Members of the receptor tyrosine kinase family, which include epidermal growth factor receptor (EGFR), ErbB-2/HER-2, ErbB-3/HER-3, and ErbB-4/HER-4, have frequently been implicated in experimental models of epithelial cell neoplasia in animals and in humans (Rajkumar and Gullick, 1994; Glenney 1992; Kroese et al., 2007; Porter and Vaillancourt, 1998). Moreover, many mAb products have been approved for clinical use in United states, and more are currently under clinical evaluation (Adams and Weiner, 2005). The Her-2/*neu* gene encodes a 185 kDa transmembrane protein that is a member of the type I family of growth factor receptors (Akiyama et al., 1986; Bargmann, 1986). Amplification of this gene results in the overexpression of a 185-kDa receptor tyrosine kinase which is homologous to EGF3 receptor (Coussens et al., 1985; Stern et al., 1986; Kraus et al., 1987). However, unlike EGF receptor, which binds many known ligands, no direct ligand of HER-2/*neu* has been reported (Hurwitz et al., 1995).

MAb to HER-2/*neu* (Trastuzumab/Herceptin) has been approved by the Federal Drug Administration (FDA) for the treatment of tumors that express high levels of HER-2/*neu*, and herceptin has a good therapeutic effect. However, recently, combined therapies, such as, antibody and chemotherapy, antibody and radio therapy (RIT) are being studies (Pfeiffer et al., 2007).

Molecular imaging can be defined as the *in vivo* characterization and measurement of biologic processes at the cellular and molecular levels (Massoud and Gambhir, 2003). The strategy of molecular imaging involves the use of unique molecular probes that target specific molecules, such as, receptors, transporters, or enzymes (Sakiyama et al., 2007; Shikano et al., 2007; Alattia et al., 2007). Moreover, specificities of such interactions, delivery pharmacokinetics, and the signal-to-noise ratio of molecular probes can be characterized by molecular imaging. However, the development and validation of specific molecules is time-consuming and requires significant effort, and thus these advantages of molecular imaging are important for evaluating the specificities of potential delivery systems (Gunn et al., 2007).

In vitro and *in vivo* antibody developments are required for RIT because the biodistribution of the radioconjugated antibody and its targeting ability should be confirmed. Nowadays, antibody development studies are performed by small animal imaging, because small animal imaging enables accurate quantification, the localizations of biological processes and events, new developed antibodies to be characterized before human studies, and because it provides near perfectly registered images which improve interpretation and quantification (Jacobs and Cherry, 2001).

Here, we report our evaluation of the merits of anti-HER-2/*neu* antibody based on small animal imaging. Our study provides information about the *in vivo* characteristics of anti-HER-2/*neu* mAb and provides supportive pre-clinical data for clinical applications.

MATERIALS AND METHODS

Materials

Erbitux (Cetuximab) was purchased from Merck Inc. (Germany), Herceptin (Trastuzumab) from Roche Inc. (USA), and IRDye 800CW from Li-Cor Inc. (USA). Fluorescein isothiocyanate (FITC), IODO-Bead and desalting dextran column were obtained from pierce (USA) and Vivaspin 500 from Vivagen (Germany). ^{125}I was from Perkin Elmer (USA), and ^{131}I from the Korean Atomic Energy Research Institute (KAERI, Korea). Phosphate buffered saline (pH 7.4; 0.01 mol/l), Dulbecco's phosphate buffered saline (pH 7.4) and casein blocker were purchased from Biorad (USA).

Preparation of radioiodine labeled antibody

Iodination of the antibody was accomplished using Iodo-Beads. A single Iodo-Bead was washed with 0.5 ml of 0.2 mol/l phosphate buffer (pH 6.5) and dried on filter paper, and then placed in an eppendorf tube. 1 mCi of radioiodine and an equal volume of 0.2 mol/l phosphate buffer (pH 6.5) was added, incubated for 15 minutes at room temperature (25℃). 200 μg of antibody was then added and incubation continued for 30 minutes at room temperature (25℃). The reaction was terminated by removing the Iodo-Bead. Labeling yield was determined by radio thin layer chromatography using silica coated glass and acetone as a developing solution.

Labeling of antibody with near-infrared fluorescence IRDye 800CW

IRDye 800CW fluorescent conjugates have an absorption maximum at 774 nm and an emission maximum of 789 nm in 1X PBS. IRDye 800CW dye bears a NHS ester reactive group that couple to primary amines on the antibody. IRDye 800CW (0.1 mg for 1 mg of protein) was dissolved in 50 μl of DMSO (Sigma, USA), 1 mg of antibody was added, and incubated overnight at 4℃ in the dark. The reaction mixture was then passed through a desalting dextran column (Pierce, USA) eluted and with 0.01 mol/l phosphate buffered saline (pH 7.4) (Biorad, USA). Fractions were concentrated by ultracentrifugation (Beckman Coulter, USA), and the product so obtained was diluted in PBS to a concentration of 1 mg/ml and stored in the dark at -20℃ until required.

Cell line and cell culture

Mouse colorectal adenocarcinoma CT-26 and HER-2/*neu* CT-26 cells were obtained from the Laboratory of Immunology at Seoul National University. CT-26 and HER-2/*neu* CT-26 cells were maintained as monolayer cultures in DMEM supplemented with 10% fetal bovine serum, 100 units/ml penicillin, and 100 μg/ml streptomycin in a humidified 5% CO_2 atmosphere at 37℃.

***In vitro* binding test**

All steps in the antibody binding assay were done at 4℃. Cells were washed 3 times with D-PBS (PBS (pH 7.4) without $CaCl_2$ and $MgCl_2$). 1×10^6 cells were counted and incubated for 1 h with ^{125}I-labeled antibody with or without a 100-fold molar excess cold antibody, and then washed twice with casein blocker. Radioisotope was counted using a Wallac 1470 gamma counter (Wallac, Finland). To correct for radioactive decay, standards were counted simultaneously.

Experimental animal model

6- to 8-week-old female athymic nude mice (BALB/c-nu Slc, Japan) were housed five/cage and provide sterilized water. Tumor cells were harvested near confluence by incubation with 0.05% trypsin-EDTA. Cells were pelleted by centrifugation at 1,500 rpm for 3 minutes and then resuspended in serum free media. Cells ($2\sim3 \times 10^6$/animal) were implanted subcutaneous into the thighs of mice. Tumors reached roughly 1 cm in size after 4 weeks.

Gamma camera images of radiolabeled antibody in small animal models

To obtain gamma camera images, mice were injected via a tail vein with radioisotope labeled antibody. Briefly, a mouse was anesthetized with 2% isoflurane and placed gamma camera (DIACAM; Siemens, Germany). Images were acquired for 1×10^6 counts using a 4 mm pin-hole. Data was stored in a 512 × 512 pixel matrix using a digital computer and processed using a special color display without background subtraction or interpolation.

Longitudinal fluorescence optical imaging of live mice and image processing

Live animal fluorescence optical imaging was performed using the IVIS 200 (Xenogen, USA). Imaging parameters were selected and implemented using on-board Living Image 2.5 software. An ICG excitation and emission filter was used with an excitation band of 710 nm to 760 nm and a emission band of 810 nm to 875 nm. Bright field photographs were obtained in each case. Images were obtained

Reg	(mm) Start	(mm) Stop	(mm) Centroid	RF	Region Counts	Region CPM	% of Total	% of ROI
Rgn 1	1.1	20.3	10.0	0.167	107375.0	107375.0	94.05	97.73
Rgn 2	36.9	56.1	44.3	0.738	2409.0	2409.0	2.11	2.19
Bkg 1	73.5	83.1	77.7	1.294				
Rgn 3	89.2	96.2	92.5	1.541	86.0	86.0	0.08	0.08
3 Peaks					109870.0	109870.0	96.23	100.00

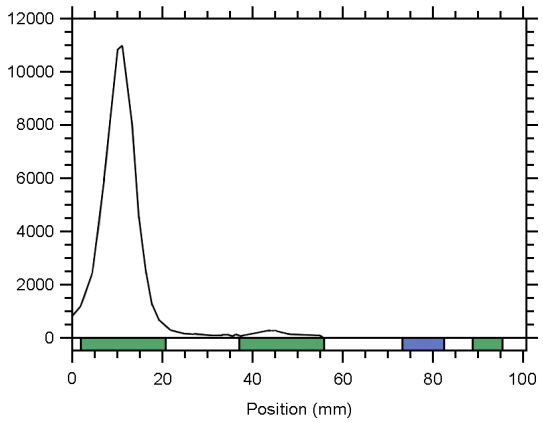

Fig. 1. Labeling efficiency of anti-HER2/*neu* antibody with ^{131}I, measured by thin layer chromatography (TLC). The labeling mixture containing antibodies, radioisotopes and chemicals were migrated on the silica coated glass buffered by acetone. Anti-HER2/*neu* antibodies were labeled with ^{131}I, demonstrating about 94% of labeling efficiency.

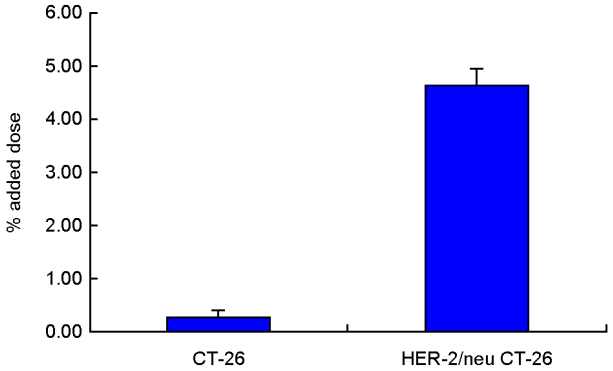

Fig. 2. *In vitro* binding assay of HER-2/*neu* CT-26 and wild-type CT-26 cell lines. Expression of HER-2/*neu* antigen is higher in HER-2/*neu* CT-26 than in wild-type CT-26. Binding % was 4.64 (±0.64) for HER-2/*neu* CT-26 and 0.26 (±0.29) for wild-type CT-26. The experiment was repeated two times.

in posterior and anterior views. Because near infrared fluorescence is susceptible with light, mouse were kept in dark room.

RESULTS

Evaluation of anti-HER2/neu mAb for radiolabeling

We assessed whether the anti-HER2/*neu* antibody could be labeled with the radioisotope. ^{131}I was used for the radiolabeling test with Iodo-bead system. The labeling efficiency was measured by radio thin layer chromatography with acetone as a developing buffer. About 94% of antibody was radiolabeled with ^{131}I (Fig. 1). This result demonstrates that the anti-HER2/*neu* antibody is suitable for radiolabeling with ^{131}I and suggests that the experiment of *in vivo* γ-camera imaging would be possible with the antibody after radio-labeling.

In vitro binding assays using anti-HER-2/*neu* mAb

To evaluate expressions of HER-2/*neu* antigens in HER-2/*neu* CT-26 and wild-type CT-26 cells, *in vitro* cell binding assays were performed (Fig. 2). Anti-HER-2/*neu* mAb was labeled with ^{125}I. ^{125}I- anti-HER-2/*neu* mAb was bound to 1 × 10^6 cells of each cell line. The binding percentage of added doses of antibody was determined by gamma counter analysis. This experiment was repeated two times. More than 20 times of radioactivity remained in HER-2/*neu* CT-26 compared to wild-type CT26. 4.64% (±0.64) of added dose is measured with HER-2/*neu* CT-26 and 0.26 (±0.29) with wild-type CT-26. In this study, we determined that HER-2/*neu* CT-26 cells possessed more antigens than wild-type CT-26.

Gamma camera imaging using ^{131}I-anti-HER-2/*neu* mAb

Then, we assessed the *in vivo* characteristics of anti-HER-2/*neu* antibodies with xenotransplanted mouse cancer model. HER-2/*neu* CT-26 and wild-type CT26 were injected in athymic nude mouse: HER-2/*neu* CT-26 in the right thigh and wild-type CT26 in the left. 200 μCi of ^{131}I-radiolabeled anti-HER-2/*neu* antibody were administrated intravenously and gamma camera images of the mouse were obtained at indicated time points after antibody injection; 1 h, 3 h, 20 h, 24 h and 48 h (Fig. 2). After 3 h of injection, the accumulation of ^{131}I-radiolabeled anti-HER-2/*neu* antibody appeared at the right thigh implanted HER-2/*neu* CT26 and increased until 48 h after injection. However, there was no

signal of accumulation of radio labeled antibody at wild-type CT26 implanted region until 24 h, although a slight increase of signal was observed at 48 h. These results show that *in vivo* gamma camera imaging could be possible with radio-labeled anti-HER-2/*neu* monoclonal antibody as the antibody binds preferentially to HER-2/*neu* antigen expressed tumor even *in vivo*.

Near infrared optical imaging using IRDye 800CW-anti-HER-2/*neu* mAb

Next, we evaluate the potential use of anti-HER-2/*neu* antibody for *in vivo* fluorescence imaging. We chose a near infrared fluorechrome, IRDye 800CW, which has an emission wavelength of 794 nm. Anti-HER-2/*neu* antibody was conjugated to the near infrared fluorescence and injected into a mouse bearing HER-2/*neu* CT26 tumor and wild-type CT26 tumor. Following anesthetization with 2% isoflurane, the mice were scanned using the IVIS 200 at various time points. The obtained images were constructed and normalized with Living image 3D software. At the time point of 1 h, the signals started appearing in either tumor regions, even slightly higher level in wild-type CT26 tumor region, and more obvious fluorescent signals appeared in either tumor regions at 3 h, and these simultaneous signals were maintained and enhanced until 24 h. However, at 48 h, the signal of wild-type CT26 tumor diminished, while that of

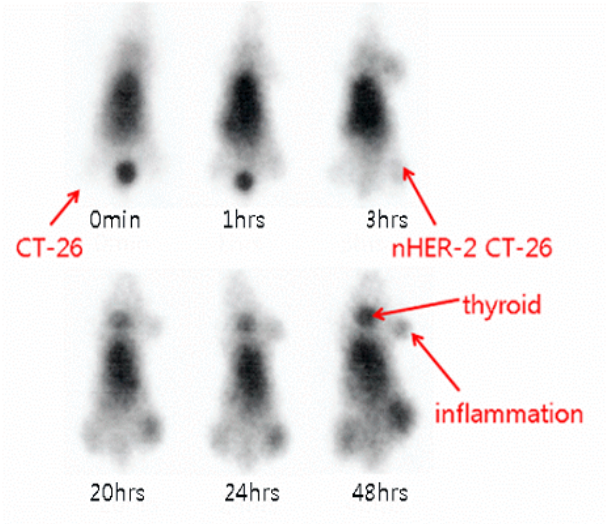

Fig. 3. Gamma camera image of tumor bearing animal model. The left thigh contained a wild-type CT-26 tumor and the right thigh a HER-2/*neu* CT-26 tumor. Anti-HER-2/*neu* mAb was labeled with ^{131}I. The image was obtained using a 4 mm pin-hole and a 512 × 512 matrix. At 20 h *p.i.*, ^{131}I-anti-HER-2/*neu* mAb accumulated in the HER-2/*neu* CT-26 tumor region, and with time, radioactivity in the HER-2/*neu* CT-26 tumor region became more increased than in the wild-type CT-26 tumor region.

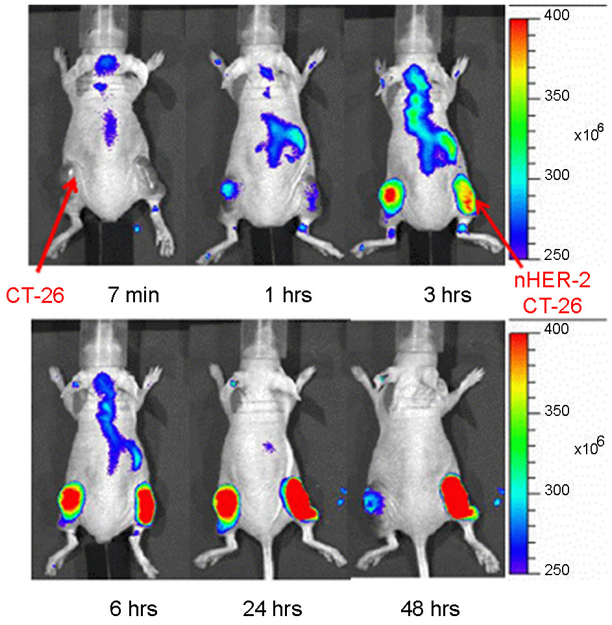

Fig. 4. Direct comparison of near infrared fluorescence imaging of HER-2/*neu* CT-26 and wild-type CT-26. Anti-HER-2/*neu* mAb was labeled with IRDye 800CW, near infrared fluorescence dye. Each image was normalized by Living 3D image software. Image was acquired from 7 min to 48 h *p.i.*.

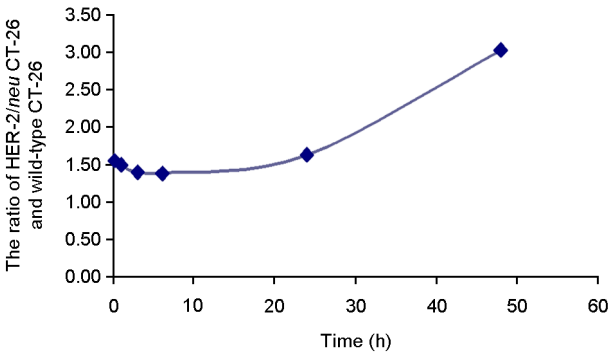

Fig. 5. HER-2/*neu* CT-26 to wild-type CT-26 ratios in near infrared fluorescence images. ROIs were drawn in tumor region using the Living Image 3D program. The HER-2/*neu* CT-26 to wild-type CT-26 ratio was 1.56 at 5 min and 3.04 at 48 h, and this ratio rapidly increased at 24 h *p.i.*.

HER-2/*neu* CT26 tumor persisted. The ratio of fluorescent signal between the regions of HER-2/*neu* CT-26 and wild-type CT-26 by ROI analysis of tumor region are shown in Fig. 5. HER-2/*neu* CT-26 and wild-type CT-26 ratios clearly increased from 1.56 at 5 min *p.i.* to 3.04 at 48 h *p.i.*, indicating the preferential binding of IRDye 800CW-anti-HER-2/*neu* antibody to HER-2/*neu* CT-26 tumor.

DISCUSSION

A cancer specific marker (or antigen) is an important element for the characterization of cancer and the development of cancer treatment modality. Despite the complexities of the nature of cancer specific markers, targeting a cancer specific marker being expressed on the surface of cancer by a specific ligand, could allow diagnosing a stage of cancer and providing treatment methods. Especially, the cancer specific markers could be used for *in vivo* imaging. Patients with breast cancer that overexpress HER-2/*neu* have a significantly lower survival rate and a shorter time to relapse (Slamon et al., 1987). Also, high levels of HER-2/*neu* expression have been positively correlated with lymph node metastasis in breast cancer (Lacroix et al., 1989; Tan et al., 1997). Some studies have suggested that high level HER-2/*neu* expressions are positively correlated with resistance to certain anti-cancer drugs and radiation-therapies (Yu et al., 1998; Arteaga et al., 1994).

The radioimmunotherapy (RIT) is a good example of treatment using cancer specific marker. RIT is a form of targeted therapy that uses parent mAbs to deliver radioactivity, which is emitted by a conjugated radioisotope, to antigen positive tissues (Kraeber-Bodéré et al., 2014). Tumor cells are damaged by the combined effects of the antibody and ionizing radiation (Read et al., 2014). During the past years, the U.S. Food and Drug Administration approved two RIT pharmaceuticals for the treatment of non-Hodgkin's lymphoma, i.e., the anti-CD20 monoclonal antibodies, ^{90}Y-ibritumomab tiuxetan (Zevalin) and ^{131}I-tositumomab (Bexxar). Moreover, several new radioimmunoconjugates are currently being evaluated in clinical trials (Sharkey and Goldenberg, 2005). The monoclonal antibody to HER-2/*neu*, Trastuzumab/Herceptin, has been approved by Federal Drug Administration (FDA) for the treatment of tumors that express high levels of HER-2/*neu* and it has a good therapeutic effect. However, combined therapies, such as, antibody and chemotherapy, antibody and radio therapy (RIT) have been studied (Pfeiffer et al., 2007).

In order to evaluate the potential use of HER-2/*neu* antigen and its ligand anti-HER-2/*neu* mAb for *in vivo* imaging, we studied *in vivo* and *in vitro* characteristics of an anti-HER-2/*neu* monoclonal antibody. First of all, we tested if the anti-HER-2/*neu* antibody can be labeled with radioisotopes. Iodo-bead method was used for preparing radioiodine labeled antibody. As seen in Fig. 1, the antibody was successfully labeled with ^{131}I and the labeling efficiency was 94% after thin layer chromatography (TLC) verification. Then, the binding ability of radiolabeled antibody to HER-2/*neu* antigen was tested. The HER-2/*neu* expressing cancer cell line, HER-2/*neu* CT26 was incubated with ^{125}I-labeled antibody, and after washing, the remaining radioactivity was measured by using a gamma counter. More than 20 times of radioactivity are measured with HER-2/*neu* expressing CT26, compared to control cell line, CT26 (Fig. 2). Although it was not possible to show statistical meaning, because of

Table 1. The nuclear properties of radioiodine isotopes

Radio nuclide	Physycal half life	Mode of decay (gamma Energy)	Possible application
I-123	13.2 hours	Electron capture (159 KeV)	Imaging (SPECT)
I-124	4.2 days	Beta + (511 KeV)	Imaging (PET)
I-125	60 days	Electron capture (X ray: 34 KeV)	In vitro and imaging
I-131	8 days	Beta - (364 KeV) (Beta rays for therapy)	Imaging (SPECT), therapy

SPECT = Single Photon Emisstion Computed Tomography, Gamma Camera
PET = Positron Emission Tomography

Table 2. Spectral properties of representative fluorescence dyes

Fluorescence dye	Excitation wavelength	Emission wavelength	Possible application
FITC	493 nm	518 nm	In vitro
Texas Red	593 nm	618 nm	In vitro
Cy 5.5	692 nm	712 nm	In vitro and In vivo
ICG (IRdye 800)	777 nm	794 nm	In vitro and In vivo

a limitation of experiments, this result could demonstrate that the radiolabeled antibody is able to interact specifically with HER-2/*neu* antigen. We have used 2 different radioiodines to verify if antibody labeling is influenced by different type of radioiodines. The antibody was successfully labeled with two different radioiodines with almost same efficacy (data not shown). As described in Table 1, there are various types of radioiodine that can be used according to needs. ^{124}I is used for PET (positron emission tomography) imaging and kinetic modeling evaluations because it emits positrons, whereas ^{131}I emits the gamma-photons and β-particles, which allow it to be used for imaging and therapy (Buchsbaum et al., 1993; Kaminski et al., 1992). It seems to be important to verify if an antibody could be labeled with various probes. Since anti-HER-2/*neu* antibody is feasible for labeling with radio-iodine and fluorescent probes, two modalities of *in vivo* imaging could be used.

The *in vivo* specific targeting of anti-HER-2/*neu* mAb was tested through the radio- and fluorescent imaging. Consistent with *in vitro* findings, specific targeting of ^{131}I-anti-HER-2/*neu* mAb to HER-2/*neu* antigen was demonstrated in tumor bearing animal model (Fig. 3). The gamma camera images of mice bearing HER-2/*neu* CT-26 tumors and wild-type CT-26 tumors demonstrated that the accumulations of ^{131}I were obvious in HER-2/*neu* CT-26 tumors but not in wild type tumors (Fig. 3). Uptake ratios between HER-2/*neu* CT-26 and CT-26 (HER-2/*neu* CT-26 to CT-26) started to increase slightly at the time point of 3 h. This increase was clearer at 20 h and maximized at 48 h (Fig. 3). Also, HER-2/*neu* CT-26 specific antibody binding was tested with *in vivo* fluorescent images. Specific binding of IRDye 800CW (a near infrared fluorescing dye) labeled anti-HER-2/*neu* mAb showed markedly more fluorescence at HER-2/*neu* expressing tumor than the wild-type tumor (Fig. 4). Since the fluorchromes with short emission wavelength, FITC, Texas Red, have some limitations for *in vivo* imaging, IRDye 800CW was used. This near infrared flourchrome has a longer emission wavelength even than Cy5.5, which is generally used for *in vivo* imaging with an emission wavelength of 712 nm (Table 2). As expected, significant fluorescent signals appeared at 3 h after antibody injection in the both tumors, even, wild type tumor showed a stronger signal. But, after 6 h, strong fluorescent signals appeared at HER-2/*neu* expressing tumor. This signal pattern continued until 48 h, where the wild type tumor signals were clearly decreased at 48 h time point. The increase of signal ratio of HER-2/*neu* CT-26 to CT-26 is more clearly demonstrated in Fig. 5, indicating preferential binding of IRDye 800CW-anti-HER-2/*neu* antibody to HER-2/*neu* CT-26 tumor. With all these *in vivo* imaging data, we could visually analyze the specific biodistribution of the injected antibody. Also, it is important to note that the increased localization of antibodies in HER-2/*neu* CT-26 region about 24 h after injection was observed even by 2 different imaging modalities. This may indicate that the localization of antibodies we observed was a real *in vivo* behavior of the antibody. In conclusion, our study demonstrates and confirms clearly that *in vivo* imaging technique is suitable for this purpose, as we characterized anti-HER-2/*neu* antibody.

Acknowledgements

This study was supported by the Semyung University Research Grant of 2012.

REFERENCES

Adams GP, Weiner LM. Monoclonal antibody therapy of cancer. Nat Biotechnol. 2005. 23: 1147-1157.

Akiyama T, Sudo C, Ogawara H, Toyoshima K, Yamamoto T. The product of the human c-erbB-2 gene: a 185-kilodalton glycoprotein with tyrosine kinase activity. Science. 1986. 232: 1644-1646.

Alattia JR, Shaw JE, Yip CM, Privé GG. Molecular imaging of membrane interfaces reveals mode of beta-glucosidase activation by saposin C. Proc Natl Acad Sci U S A. 2007. 104: 17394-17399.

Arteaga CL, Winnier AR, Poirier MC, Lopez-Larraza DM, Shawver LK, Hurd SD, Stewart SJ. p185c-erbB-2 signal enhances cisplatin-induced cytotoxicity in human breast carcinoma cells: association between an oncogenic receptor tyrosine kinase and drug-induced DNA repair. Cancer Res. 1994. 54: 3758 -3765.

Bargmann CI, Hung MC, Weinberg RA. The neu oncogene encodes an epidermal growth factor receptor-related protein. Nature. 1986. 319: 226-230.

Buchsbaum DJ, Langmuir VK, Wessels BW. Experimental radioimmunotherapy. Med Phys. 1993. 20: 551-567.

Coussens L, Yang-Feng TL, Liao YC, Chen E, Gray A, McGrath J, Seeburg PH, Libermann TA, Schlessinger J, Francke U, Levinson A, Axel Ullrich. Tyrosine kinase receptor with extensive homology to EGF receptor shares chromosomal location with neu oncogene. Science. 1985. 230: 1132-1139.

Crawford LM Jr. From the Food and Drug Administration. JAMA. 2002. 288: 1579.

DeNardo GL, DeNardo SJ, O'Donnell RT, Kroger LA, Kukis DL, Meares CF, Goldstein DS, Shen S. Are radiometal-labeled antibodies better than iodine-131-labeled antibodies: comparative pharmacokinetics and dosimetry of copper-67-, iodine-131-, and yttrium-90-labeled Lym-1 antibody in patients with non-Hodgkin's lymphoma. Clin Lymphoma. 2000. 1: 118-126.

DeNardo GL, Kukis DL, Shen S, DeNardo DA, Meares CF, DeNardo SJ. ^{67}Cu-versus ^{131}I-labeled Lym-1 antibody: comparative pharmacokinetics and dosimetry in patients with non-Hodgkin's lymphoma. Clin Cancer Res. 1999. 5: 533-541.

Esteban JM, Hyams DM, Beatty BG, Merchant B, Beatty JD. Radioimmunotherapy of human colon carcinomatosis xenograft with ^{90}Y-ZCE025 monoclonal antibody: toxicity and tumor phenotype studies. Cancer Res. 1990. 50: 989s-992s.

Fani M, Vranjes S, Archimandritis SC, Potamianos S, Xanthopoulos S, Bouziotis P, Varvarigou AD. Labeling of monoclonal antibodies with ^{153}Sm for potential use in radioimmunotherapy. Appl Radiat Isot. 2002. 57: 665-674.

Glenney JR Jr. Tyrosine-phosphorylated proteins: mediators of signal transduction from the tyrosine kinases. Biochim Biophys Acta. 1992. 1134: 113-127.

Gunn AJ, Brechbiel MW, Choyke PL. The emerging role of molecular imaging and targeted therapeutics in peritoneal carcinomatosis. Expert Opin Drug Deliv. 2007. 4: 389-402.

Hurwitz E, Stancovski I, Sela M, Yarden Y. Suppression and promotion of tumor growth by monoclonal antibodies to ErbB-2 differentially correlate with cellular uptake. Proc Natl Acad Sci U S A. 1995. 92: 3353-3357.

Jacobs RE, Cherry SR. Complementary emerging techniques: high-resolution PET and MRI. Curr Opin Neurobiol. 2001. 11: 621 -629.

Jaramillo ML, Leon Z, Grothe S, Paul-Roc B, Abulrob A, O'Connor McCourt M. Effect of the anti-receptor ligand-blocking 225 monoclonal antibody on EGF receptor endocytosis and sorting. Exp Cell Res. 2006. 312: 2778-2790.

Kaminski MS, Fig LM, Zasadny KR, Koral KF, DelRosario RB, Francis IR, Hanson CA, Normolle DP, Mudgett E, Liu CP, Moon S, Scott P, Miller RA, Wahl RL. Imaging, dosimetry, and radioimmunotherapy with iodine 131-labeled anti-CD37 antibody in B-cell lymphoma. J Clin Oncol. 1992. 10: 1696 -1711.

Kraeber-Bodéré F, Bodet-Milin C, Rousseau C, Eugène T, Pallardy A, Frampas E, Carlier T, Ferrer L, Gaschet J, Davodeau F, Gestin JF, Faivre-Chauvet A, Barbet J, Chérel M. Radioimmunoconjugates for the treatment of cancer. Semin Oncol. 2014. 41: 613-622.

Krose M, Zimmern RL, Pinder SE. HER2 status in breast cancer--an example of pharmacogenetic testing. J R Soc Med. 2007. 100: 326-329.

Kraus MH, Popescu NC, Amsbaugh SC, King CR. Overexpression of the EGF receptor-related proto-oncogene erbB-2 in human mammary tumor cell lines by different molecular mechanisms. EMBO J. 1987. 6: 605-610.

Lacroix H, Iglehart JD, Skinner MA, Kraus MH. Overexpression of erbB-2 or EGF receptor proteins present in early stage mammary carcinoma is detected simultaneously in matched primary tumors and regional metastases. Oncogene. 1989. 4: 145-151.

Lewington V. Development of ^{131}I-tositumomab. Semin Oncol. 2005. 32: S50-S56.

Massoud TF, Gambhir SS. Molecular imaging in living subjects: seeing fundamental biological processes in a new light. Genes Dev. 2003. 17: 545-580.

Pfeiffer P, Nielsen D, Yilmaz M, Iversen A, Vejlø C, Jensen BV.

Cetuximab and irinotecan as third line therapy in patients with advanced colorectal cancer after failure of irinotecan, oxaliplatin and 5-fluorouracil. Acta Oncol. 2007. 46: 697-701.

Porter AC, Vaillancourt RR. Tyrosine kinase receptor-activated signal transduction pathways which lead to oncogenesis. Oncogene. 1998. 17: 1343-1352.

Rajkumar T, Gullick WJ. The type I growth factor receptors in human breast cancer. Breast Cancer Res Treat. 1994. 29: 3-9.

Read ED, Eu P, Little PJ, Piva TJ. The status of radioimmunotherapy in CD20+ non-Hodgkin's lymphoma. Target Oncol. 2015. 10: 15-26.

Richman CM, DeNardo SJ. Systemic radiotherapy in metastatic breast cancer using ^{90}Y-linked monoclonal MUC-1 antibodies. Crit Rev Oncol Hematol. 2001. 38: 25-35.

Sakiyama Y, Hatano K, Tajima T, Kato T, Kawasumi Y, Suzuki M, Ito K. An atlas-based image registration method for dopamine receptor imaging with PET in rats. Ann Nucl Med. 2007. 21: 455-462.

Sharkey RM, Goldenberg DM. Perspectives on cancer therapy with radiolabeled monoclonal antibodies. J Nucl Med. 2005. 46: 115-127.

Shikano N, Nakajima S, Kotani T, Ogura M, Sagara J, Iwamura Y, Yoshimoto M, Kubota N, Ishikawa N, Kawai K. Transport of D-[1-14C]-amino acids into Chinese hamster ovary (CHO-K1) cells: implications for use of labeled d-amino acids as molecular imaging agents. Nucl Med Biol. 2007. 34: 659-665.

Shimoni A, Nagler A. Radioimmunotherapy and stem-cell transplantation in the treatment of aggressive B-cell lymphoma. Leuk Lymphoma. 2007. 48: 2110-2120.

Slamon DJ, Clark GM, Wong SG, Levin WJ, Ullrich A, McGuire WL. Human breast cancer: correlation of relapse and survival with amplification of the HER-2/*neu* oncogene. Science. 1987. 235: 177-182.

Stern DF, Heffernan PA, Weinberg RA. p185, a product of the neu proto-oncogene, is a receptorlike protein associated with tyrosine kinase activity. Mol Cell Biol. 1986. 6: 1729-1740.

Tan M, Yao J, Yu D. Overexpression of the c-erbB-2 gene enhanced intrinsic metastasis potential in human breast cancer cells without increasing their transformation abilities. Cancer Res. 1997. 57: 1199-1205.

van Gog FB, Visser GW, Stroomer JW, Roos JC, Snow GB, van Dongen GA. High dose rhenium-186-labeling of monoclonal antibodies for clinical application: pitfalls and solutions. Cancer. 1997. 80: 2360-2370.

Wiseman GA, White CA, Stabin M, Dunn WL, Erwin W, Dahlbom M, Raubitschek A, Karvelis K, Schultheiss T, Witzig TE, Belanger R, Spies S, Silverman DH, Berlfein JR, Ding E, Grillo-López AJ. Phase I/II ^{90}Y-Zevalin (yttrium-90 ibritumomab tiuxetan, IDEC-Y2B8) radioimmunotherapy dosimetry results in relapsed or refractory non-Hodgkin's lymphoma. Eur J Nucl Med. 2000. 27: 766-777.

Witzig TE. Radioimmunotherapy for B-cell non-Hodgkin lymphoma. Best Pract Res Clin Haematol. 2006. 19: 655-668.

Yu D, Liu B, Jing T, Sun D, Price JE, Singletary SE, Ibrahim N, Hortobagyi GN, Hung MC. Overexpression of both p185c-erbB2 and p170mdr-1 renders breast cancer cells highly resistant to taxol. Oncogene. 1998. 16: 2087-2094.